Octupole correlation in ^{67}Ga

Z. X. Zhou,[1] D. W. Luo,[1,*] H. Y. Wu,[2,1,†] Y. Y. Wang,[3] Y. F. Niu,[4] W. Zhang,[5] C. Xu,[1] G. S. Li,[6] Z. H. Li,[1] H. Hua,[1,‡] S. Q. Zhang,[1] C. Y. Guo,[1] X. Q. Li,[1] Y. H. Qiang,[6] Aman Rohilla,[6] J. Lin,[1] J. Z. Zhang,[1] L. Ni,[1] S. Y. Zhang,[1] J. G. Wang,[6] Y. D. Fang,[6] M. Kumar Raju,[6,7] D. Bing,[6] W. Q. Zhang,[6] H. Huang,[6] M. L. Liu,[6] F. F. Zeng,[6] S. Guo,[6] and X. H. Zhou[6]

[1]*School of Physics and State Key Laboratory of Nuclear Physics and Technology, Peking University, Beijing 100871, China*

[2]*Key Laboratory of Nuclear Data, China Institute of Atomic Energy, Beijing 102413, China*

[3]*Mathematics and Physics Department, North China Electric Power University, Beijing 102206, China*

[4]*School of Nuclear Science and Technology, Lanzhou University, Lanzhou 730000, China*

[5]*School of Physics and Microelectronics, Zhengzhou University, Zhengzhou 450001, China*

[6]*Institute of Modern Physics, Chinese Academy of Sciences, Lanzhou 730000, China*

[7]*Department of Physics, GITAM School of Science, Visakhapatnam 530045, India*

(Received 6 December 2023; revised 6 May 2024; accepted 25 July 2024; published 12 August 2024)

High-spin states of ^{67}Ga have been studied via the ^{58}Ni(^{12}C, $3p$)^{67}Ga fusion-evaporation reaction at a beam energy of 50.4 MeV. Three negative-parity bands and three positive-parity bands in ^{67}Ga are established. The observation of one new $E3$ transition linking the positive-parity $\pi 1g_{9/2}$ band and negative-parity $\pi 2p_{3/2}$ band provides evidence of octupole correlations in ^{67}Ga. The characteristics of octupole correlations in the ^{67}Ga are discussed in terms of the reflection-asymmetric triaxial particle rotor model and microscopic relativistic mean field + Bardeen-Cooper-Schrieffer model.

DOI: 10.1103/PhysRevC.110.024309

I. INTRODUCTION

With the breaking of reflection symmetry in the intrinsic frame, some nuclei appear to have an octupole deformation [1,2]. The occurrence of octupole deformations can be ascribed to the interaction between an intruder orbital and the normal parity subshell which differ by three units of angular momentum. The explorations of strong octupole effects throughout the nuclear chart have long been of great interest in nuclear structure physics. To date, the well-known nuclear regions with the octupole deformation are around the double octupole driving numbers $Z = 56$, $N = 88$ and $Z = 88$, $N = 134$, where the experimental evidences of octupole deformation or correlations have been identified in many nuclei [3–5].

Recently, particular attention has been paid to nuclei in the $A \approx 70$ mass region, which is around the double octupole driving numbers $Z = N = 34$. Since this region is situated in a gradual shape transition from spherical to deformed along the isospin chain, octupole correlations are expected to spread over several nucleon numbers. For example, octupole correlations between multiple chiral doublet bands have been observed in ^{78}Br ($Z = 35$, $N = 43$) [6] and an octupole rotational band has been observed in ^{71}Ge ($Z = 32$, $N = 39$) [7]. In spite of some progress made, the information on octupole properties in this region is still scarce. It is of interest to further probe the octupole effects in this region.

In general, the experimental fingerprints of octupole correlations [2] are the observation of enhanced $E3$ and/or $E1$ transitions linking the excited bands to alternating opposite-parity yrast bands. In the $A \approx 70$ region, octupole correlations are associated with the $g_{9/2}$ and $p_{3/2}$ subshells. Here, we report an experimental investigation of the collective structures in ^{67}Ga via the ^{58}Ni(^{12}C, $3p$)^{67}Ga fusion-evaporation reaction. Three negative-parity bands and three positive-parity bands in ^{67}Ga are established. The observation of one new $E3$ transition linking the positive-parity $\pi 1g_{9/2}$ band and negative-parity $\pi 2p_{3/2}$ band provides evidence of octupole correlations in ^{67}Ga. The characteristics of octupole correlations in the ^{67}Ga are discussed in terms of the reflection-asymmetric triaxial particle rotor model (RAT-PRM) [8,9] and microscopic relativistic mean field + Bardeen-Cooper-Schrieffer model (RMF+BCS) [10–12].

II. EXPERIMENT

The present experiment was performed at the Heavy Ion Research Facility in Lanzhou, China. High-spin states of ^{67}Ga were populated via the ^{58}Ni(^{12}C, $3p$)^{67}Ga fusion-evaporation reaction at 50.4 MeV beam energy. The ^{58}Ni target with a thickness of 0.92 mg/cm^2 on 9.4 mg/cm^2 Au backing was used. The in-beam γ rays were detected by a detection array which consisted of seven segmented clover detectors and 14 high-purity germanium (HPGe) with bismuth germinate (BGO) anti-Compton suppressors. All the clover detectors were placed in a ring perpendicular to the beam. The 14 HPGe detectors were placed in five different angles at 26°, 52°, 90°, 128°, and 154° with respect to the beam direction.

*Contact author: luodiwen@pku.edu.cn
†Contact author: wuhongyi@pku.edu.cn
‡Contact author: hhua@pku.edu.cn

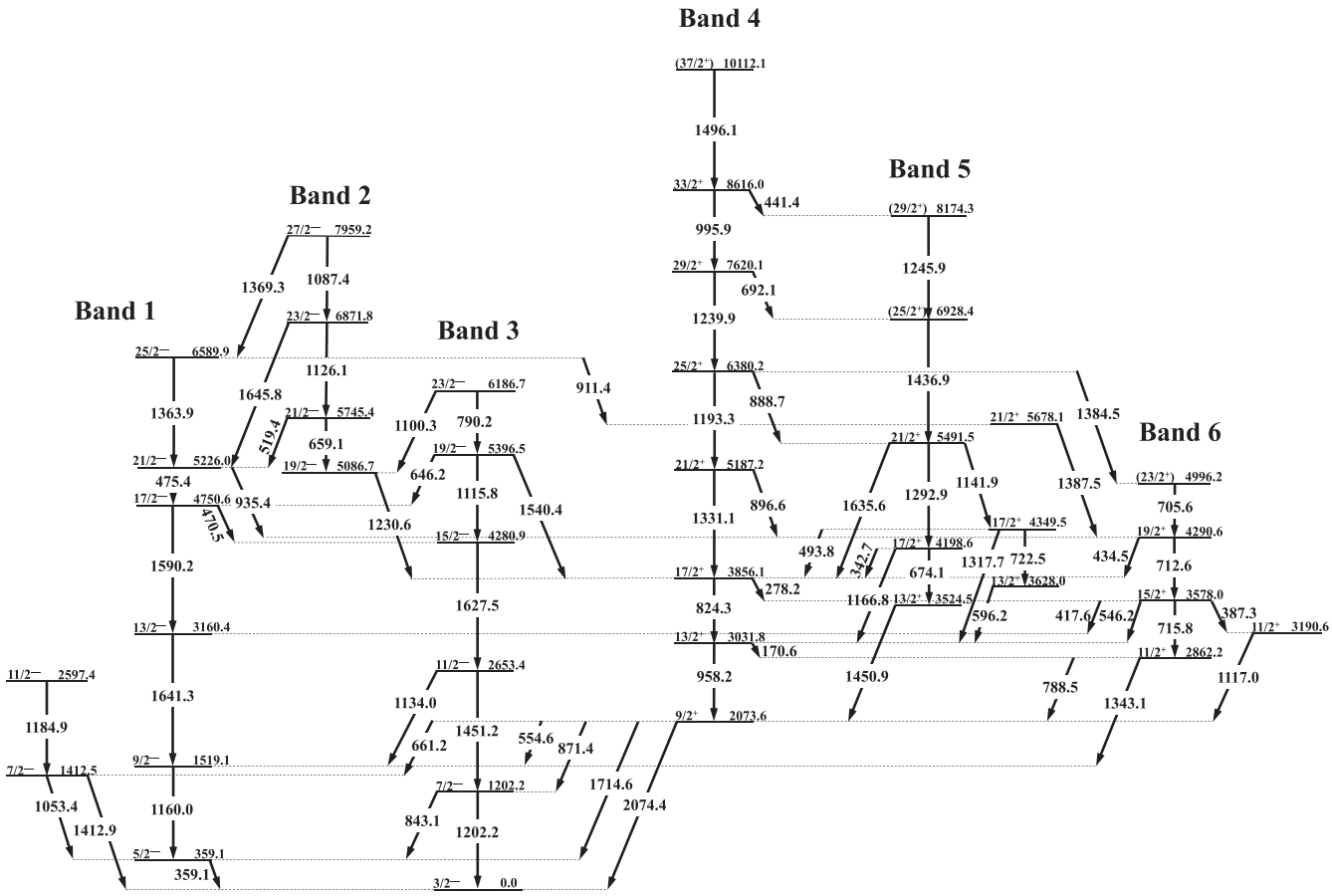

FIG. 1. Partial level scheme of ^{67}Ga energies are in keV.

All the detectors were calibrated using the standard ^{152}Eu and ^{133}Ba γ-ray sources. Approximately 1.9×10^9 γ-γ coincident events were collected, from which a γ-γ symmetric matrix and a γ-γ-γ cube were built. The level scheme analysis was performed using the RADWARE package [13] and the Cubix software [14]. To determine the multipolarities of the γ-ray transitions, two asymmetric angular distributions from oriented states (ADO) [15] matrices were constructed by using the γ rays detected at all angles (the y axis) against those detected at 90° and 26° + 154° (the x axis), respectively. The multipolarities of the emitted γ rays were analyzed by means of the ADO ratio, defined as $[I_\gamma(26°) + I_\gamma(154°)]/I_\gamma(90°)$. In general, the typical ADO ratios for the stretched quadrupole and stretched pure dipole transitions are found to be ≈0.9 and ≈0.5, respectively.

III. RESULTS AND DISCUSSION

With three protons outside the ^{56}Ni doubly magic core, it has been known that the low-lying negative-parity $1/2^-$, $3/2^-$, and $5/2^-$ states in the odd-A Ga isotopes are associated with the $2p_{1/2}$, $2p_{3/2}$, and $1f_{5/2}$ proton orbitals, respectively, while the low-lying positive-parity $9/2^+$ state originates from the unpaired proton occupying the $1g_{9/2}$ orbit [16–19]. For the ^{67}Ga, its collective structures have been previously studied by many experiments, including ^{64}Zn(α, p)^{67}Ga [20–22], ^{53}Cr(^{16}O, pn)^{67}Ga [22], ^{57}Fe(^{12}C, pn)^{67}Ga [23], ^{12}C(^{58}Ni, $3p$)^{67}Ga [17], and ^{46}Ti(^{25}Mg, $3pn$)^{67}Ga [16] fusion evaporation reactions. Two negative-parity bands built on the $2p_{3/2}$ and $1f_{5/2}$ proton orbitals, respectively, and one positive-parity band built on the $1g_{9/2}$ proton orbital, have been reported [24].

The partial level scheme of ^{67}Ga deduced from the present work is shown in Fig. 1. Three negative-parity bands and three positive-parity bands are established. They were constructed from the γ-γ coincidence relationships, intensity balances, and ADO ratios. The results are summarized in Table I. The ADO ratios are plotted as a function of γ-ray energy for most of the observed transitions in ^{67}Ga in Fig. 2. Typical γ-ray spectra with double and single gates on the low-lying transitions in ^{67}Ga are shown in Figs. 3 and 4, respectively. The present analyses confirm the transitions found in the previous studies and support their spin-parity assignments.

The negative-parity band 1 built on the $\pi 1f_{5/2}$ orbital is extended up to the same levels as in Ref. [17]. For the negative-parity band 3 built on the $\pi 2p_{3/2}$ orbital, although the $19/2^-$ level at 5396.5 keV was identified, the $E2$ transition of 1115.8 keV from $19/2^-$ level to $15/2^-$ level was not observed previously [17]. Here, with the gate on 1202.2-keV transition, the γ ray of 1115.8 keV can be seen in Fig. 4(c). For the positive-parity band 4 built on the $\pi 1g_{9/2}$ orbital, in Ref. [17], a transition of 1468 keV was tentatively placed on the $33/2^+$ level. In the present work with more statistics, this 1468-keV transition is not observed, while a new 1496.1-keV transition is found to be in coincidence with the known $E2$

TABLE I. γ-ray energies, excitation energies, relative γ-ray intensities, ADO ratios, spin-parity assignments in ^{67}Ga.

E_γ(keV)	E_i(keV)	Relative intensities	$R_{\rm ADO}$	$I_i \rightarrow I_f$
170.6(3)	3031.8(2)	0.28(2)		$13/2^+ \rightarrow 11/2^+$
278.2(1)	3856.1(3)	1.77(6)	0.67(3)	$17/2^+ \rightarrow 15/2^+$
342.7(1)	4198.6(3)	10.46(30)	1.37(5)	$17/2^+ \rightarrow 17/2^+$
359.1(1)	359.1(1)	83.8(24)	0.49(2)	$5/2^- \rightarrow 3/2^-$
387.3(1)	3578.0(3)	1.42(5)	1.22(5)	$15/2^+ \rightarrow 11/2^+$
417.6(1)	3578.0(3)	1.68(6)	0.56(2)	$15/2^+ \rightarrow 13/2^-$
434.5(1)	4290.6(3)	0.73(3)	0.43(4)	$19/2^+ \rightarrow 17/2^+$
441.4(2)	8616.0(4)	0.95(3)		$33/2^+ \rightarrow (29/2^+)$
470.5(1)	4750.6(3)	0.58(11)	0.83(5)	$17/2^- \rightarrow 15/2^-$
475.4(1)	5226.0(3)	1.09(4)	1.29(16)	$21/2^- \rightarrow 17/2^-$
493.8(1)	4349.5(3)	2.42(9)	1.19(10)	$17/2^+ \rightarrow 17/2^+$
519.4(1)	5745.4(3)	1.61(7)		$21/2^- \rightarrow 21/2^-$
546.2(1)	3578.0(3)	30.45(65)	0.41(1)	$15/2^+ \rightarrow 13/2^+$
554.6(1)	2073.6(2)	40.56(87)	1.01(3)	$9/2^+ \rightarrow 9/2^-$
596.2(2)	3628.0(3)	1.54(6)		$13/2^+ \rightarrow 13/2^+$
646.2(1)	5396.5(4)	0.79(4)	0.56(3)	$19/2^- \rightarrow 17/2^-$
659.1(1)	5745.4(3)	0.56(3)		$21/2^- \rightarrow 19/2^-$
661.2(1)	2073.6(2)	0.68(6)		$9/2^+ \rightarrow 7/2^-$
674.1(3)	4198.6(3)	0.66(2)		$17/2^+ \rightarrow 13/2^+$
692.1(1)	7620.1(4)	0.47(3)	0.95(6)	$29/2^+ \rightarrow (25/2^+)$
705.6(1)	4996.2(3)	1.22(5)		$(23/2^+) \rightarrow 19/2^+$
712.6(1)	4290.6(3)	33.12(72)	1.02(3)	$19/2^+ \rightarrow 15/2^+$
715.8(1)	3578.0(3)	2.11(7)	0.99(5)	$15/2^+ \rightarrow 11/2^+$
722.5(2)	4349.5(3)	0.75(4)		$17/2^+ \rightarrow 13/2^+$
788.5(2)	2862.2(2)	0.30(2)		$11/2^+ \rightarrow 9/2^+$
790.2(1)	6186.7(4)	2.32(8)	1.14(8)	$23/2^- \rightarrow 19/2^-$
824.3(1)	3856.1(3)	41.34(90)	0.97(3)	$17/2^+ \rightarrow 13/2^+$
843.1(1)	1202.2(2)	18.82(41)	0.42(1)	$7/2^- \rightarrow 5/2^-$
871.4(1)	2073.6(2)	55.7(12)	0.45(2)	$9/2^+ \rightarrow 7/2^-$
888.7(1)	6380.2(4)	26.06(73)	0.97(3)	$25/2^+ \rightarrow 21/2^+$
896.6(1)	5187.2(3)	0.92(4)		$21/2^+ \rightarrow 19/2^+$
911.4(1)	6589.9(4)	0.66(3)		$25/2^- \rightarrow 21/2^+$
924.4(1)[a]	4780.5(3)	1.87(7)	1.25(6)	$21/2^+ \rightarrow 17/2^+$
935.4(1)	5226.0(3)	16.94(48)	0.42(1)	$21/2^- \rightarrow 19/2^+$
958.2(1)	3031.8(2)	100.00	0.94(3)	$13/2^+ \rightarrow 9/2^+$
995.9(1)	8616.0(4)	13.93(40)	0.85(3)	$33/2^+ \rightarrow 29/2^+$
1053.4(1)	1412.5(2)	1.68(7)		$7/2^- \rightarrow 5/2^-$
1069.4(1)[a]	5820.0(4)	1.55(8)	0.78(6)	$(19/2^-) \rightarrow 17/2^-$
1087.4(2)	7959.2(4)	1.33(6)	0.89(5)	$27/2^- \rightarrow 23/2^-$
1100.3(2)	6186.7(4)	1.06(4)	0.89(4)	$23/2^- \rightarrow 19/2^-$
1115.8(2)	5396.5(4)	0.55(3)	0.69(17)	$19/2^- \rightarrow 15/2^-$
1117.0(2)	3190.6(3)	1.76(6)		$11/2^+ \rightarrow 9/2^+$
1126.1(5)	6871.8(4)	0.45(2)		$23/2^- \rightarrow 21/2^-$
1134.0(2)	2653.4(2)	0.99(3)		$11/2^- \rightarrow 9/2^-$
1141.9(2)	5491.5(3)	4.97(15)	0.95(4)	$21/2^+ \rightarrow 17/2^+$
1160.0(2)	1519.1(2)	64.8(20)	0.90(3)	$9/2^- \rightarrow 5/2^-$
1166.8(2)	4198.6(3)	11.01(32)	0.84(3)	$17/2^+ \rightarrow 13/2^+$
1184.9(2)	2597.4(3)	0.51(2)		$11/2^- \rightarrow 7/2^-$
1192.6(2)[a]	5473.5(4)	0.61(4)		$(19/2^-) \rightarrow 15/2^-$
1193.3(2)	6380.2(4)	1.64(6)	0.81(19)	$25/2^+ \rightarrow 21/2^+$
1202.2(2)	1202.2(2)	60.8(14)	0.91(3)	$7/2^- \rightarrow 3/2^-$
1230.6(2)	5086.7(3)	5.20(20)	0.48(2)	$19/2^- \rightarrow 17/2^+$
1239.9(2)	7620.1(4)	21.37(62)	0.89(3)	$29/2^+ \rightarrow 25/2^+$
1245.9(3)	8174.3(4)	1.28(6)	0.98(7)	$(29/2^+) \rightarrow (25/2^+)$
1292.9(2)	5491.5(3)	14.36(42)	0.86(3)	$21/2^+ \rightarrow 17/2^+$
1317.7(2)	4349.5(3)	6.35(19)		$17/2^+ \rightarrow 13/2^+$
1331.1(2)	5187.2(3)	4.28(16)	0.88(3)	$21/2^+ \rightarrow 17/2^+$
1343.1(2)	2862.2(2)	5.37(17)	0.41(1)	$11/2^+ \rightarrow 9/2^-$
1363.9(2)	6589.9(4)	4.11(12)	0.86(4)	$25/2^- \rightarrow 21/2^-$
1369.3(2)	7959.2(4)	1.83(6)	0.76(3)	$27/2^- \rightarrow 25/2^-$
1384.5(2)	6380.2(4)	0.44(2)		$25/2^+ \rightarrow (23/2^+)$
1387.5(2)	5678.1(3)	5.33(23)		$21/2^+ \rightarrow 19/2^+$
1412.9(2)	1412.5(2)	3.16(15)		$7/2^- \rightarrow 3/2^-$
1413.0(2)[a]	6904.7(4)			$(25/2^+) \rightarrow 21/2^+$
1436.9(2)	6928.4(4)	1.69(7)	0.77(4)	$(25/2^+) \rightarrow 21/2^+$
1451.2(2)	2653.4(2)	7.09(21)	0.99(7)	$11/2^- \rightarrow 7/2^-$
1450.9(2)	3524.5(3)	0.75(3)		$13/2^+ \rightarrow 9/2^+$
1496.1(3)	10112.1(5)	4.27(17)		$(37/2^+) \rightarrow 33/2^+$
1540.4(2)	5396.5(4)	1.59(6)		$19/2^- \rightarrow 17/2^+$
1590.2(2)	4750.6(3)	3.19(10)	0.90(3)	$17/2^- \rightarrow 13/2^-$
1627.5(2)	4280.9(3)	1.58(6)	0.83(4)	$15/2^- \rightarrow 11/2^-$
1635.6(2)	5491.5(3)	10.71(31)	0.93(3)	$21/2^+ \rightarrow 17/2^+$
1641.3(2)	3160.4(3)	6.60(21)	1.45(8)	$13/2^- \rightarrow 9/2^-$
1645.8(2)	6871.8(4)	1.55(7)	0.79(3)	$23/2^- \rightarrow 21/2^-$
1714.6(2)	2073.6(2)	2.95(9)	1.01(4)	$9/2^+ \rightarrow 5/2^-$
2074.4(2)	2073.6(2)	0.23(1)		$9/2^+ \rightarrow 3/2^-$

[a]Not placed in the partial level scheme shown in Fig. 1.

transitions in band 4 shown in Fig. 4(a). This new 1496.1-keV γ ray for which the DCO ratio could not be extracted is also assumed to be a stretched $E2$ transition.

Bands 2, 5, and 6 are newly established. As shown in Fig. 3(b), by requiring coincidence with the 958.2- and 824.3-keV transitions, two new 1436.9- and 1245.9-keV transitions are observed. The observation of two cross-band 692.1- and 441.4-keV transitions gives support to the placement of these two transitions. The present ADO analyses for these two transitions and neighboring interband 692.5-keV transition suggest the new 1436.9- and 1245.9-keV transitions are $E2$ transitions.

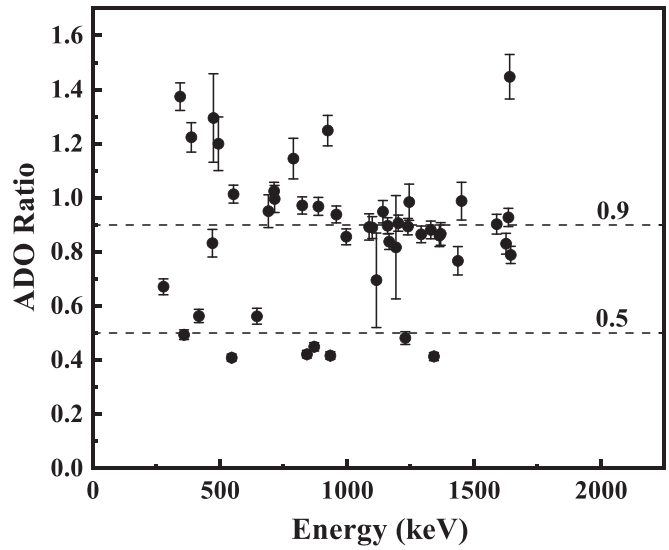

FIG. 2. The ADO ratios as a function of γ-ray energy for transitions in ^{67}Ga.

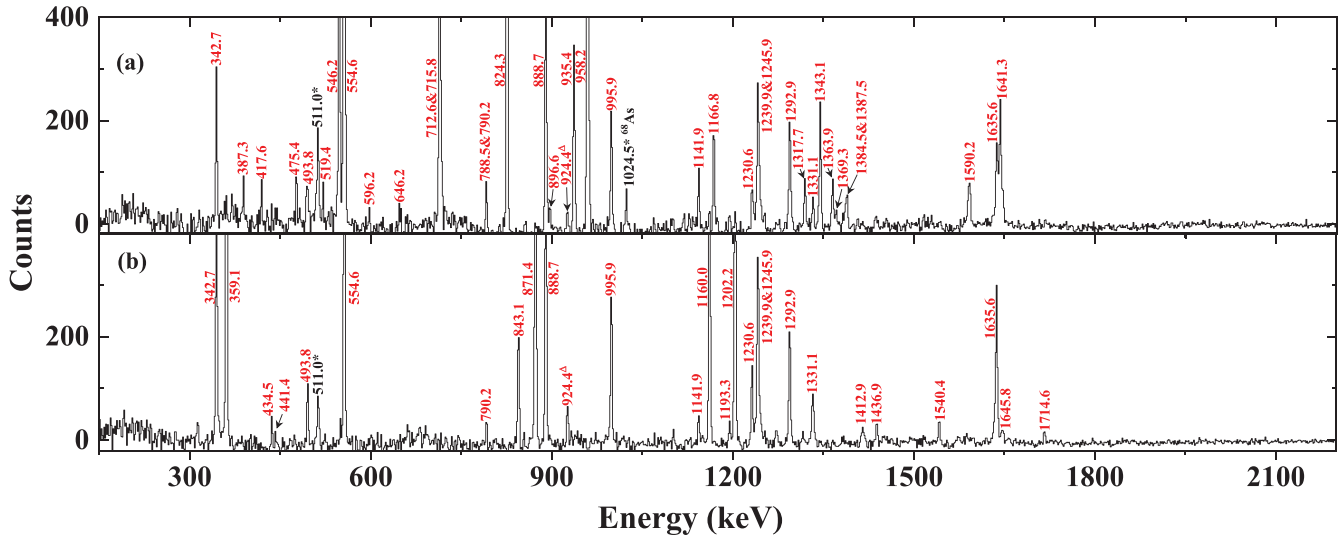

FIG. 3. Coincident γ-ray spectra double gated on the (a) 359.1- and 1160.0-keV transitions, (b) 958.2- and 824.3-keV transitions. Transitions of ^{67}Ga are marked in red. The peaks marked with asterisks are known contaminants, and the peaks marked with triangles belong to ^{67}Ga but are not included in the partial level scheme of Fig. 1.

Here, of particular interest is the observation of one new 2074.4-keV $E3$ transition linking the positive-parity $\pi 1g_{9/2}$ band and negative-parity $\pi 2p_{3/2}$ band. As shown in Fig. 4, this new 2074.4-keV $E3$ transition is in coincidence with the known γ-ray transitions of 958.2 keV and 546.2 keV and not with the 1202.2-keV transition. Also, with gate on the 2074.4-keV transition in Fig. 5, the strong transitions of 546.2, 712.6, 824.3, 888.7, and 958.2 keV in ^{67}Ga are clearly seen. But unfortunately, due to the relative weak intensity of the 2074.4-keV transition, the peak at 2074.4 keV is not clearly

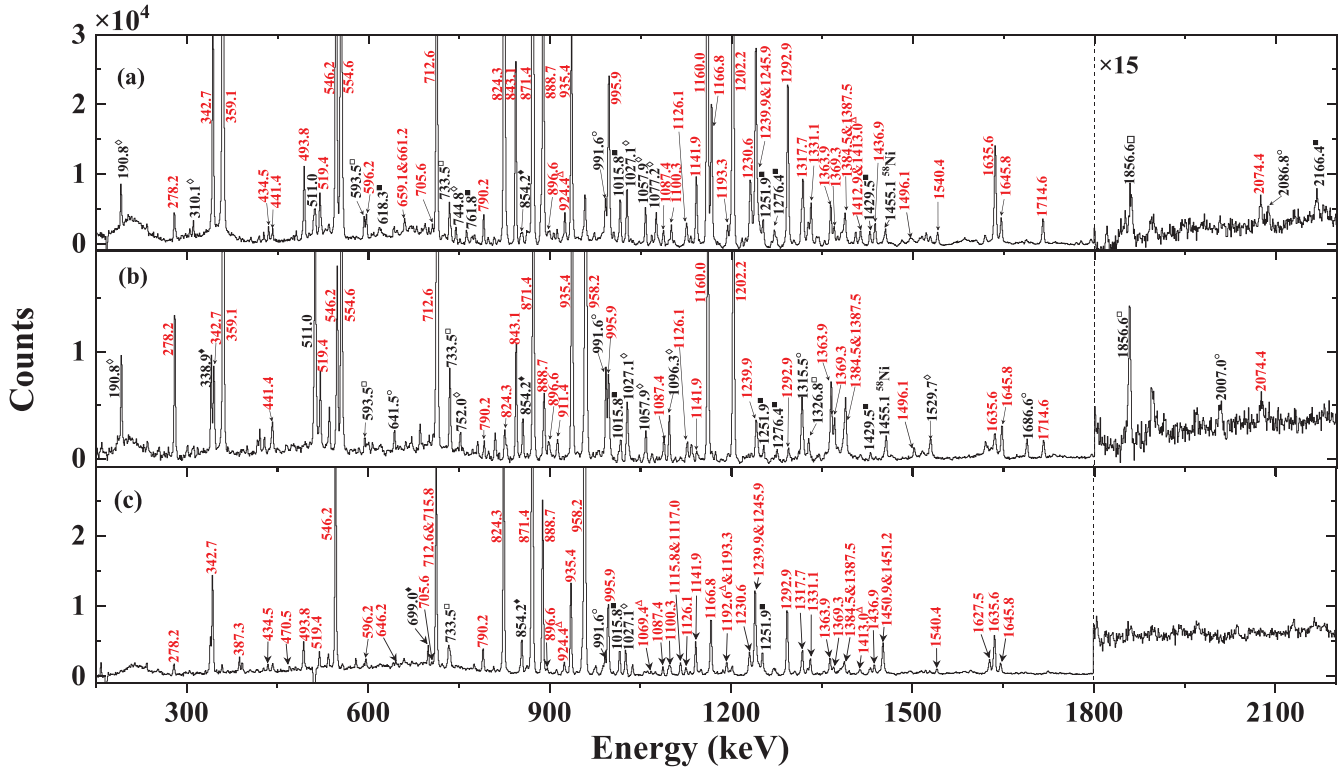

FIG. 4. Coincident γ-ray spectra gated on the (a) 958.2-keV transitions, (b) 546.2-keV transitions, and (c) 1202.2-keV transitions. Transitions of ^{67}Ga are marked in red, and the peaks marked with triangles belong to ^{67}Ga but are not included in the partial level scheme of Fig. 1. Main contaminants are marked with symbols from ^{65}Ga(◊), ^{68}As(♦), ^{67}Ge(□), ^{68}Ge(■), and ^{64}Zn(◯) via fusion-evaporation reaction.

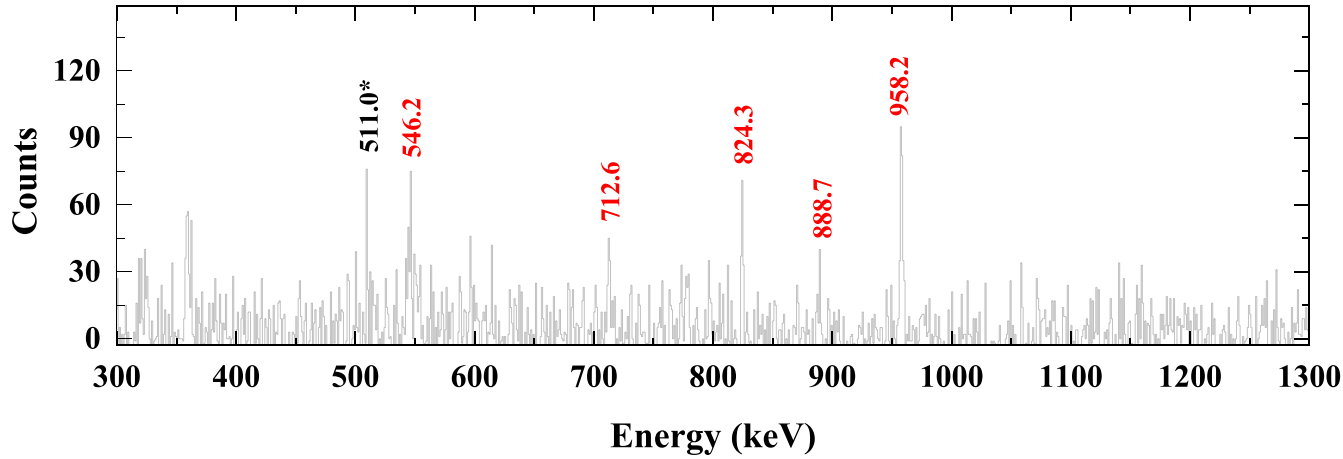

FIG. 5. Coincident γ-ray spectrum gated on the 2074.4-keV transitions in ^{67}Ga. Transitions of ^{67}Ga are marked in red.

shown in double gated γ spectrum in Fig. 3(b). It is well known that one of the experimental evidences for octupole correlations is the observation of the $E3$ transition between the opposite-parity bands. This new $E3$ transition between bands 3 and 4 indicates that the octupole correlations may exist in ^{67}Ga.

Figure 6 shows the low-lying states and the transitions populated by the $9/2^+$ states of odd-Z $^{63-71}$Ga and $^{61-69}$Cu isotopes, as well as the 3^- octupole states in the neighboring even-Z Ni and Zn isotopes. It can be seen that both excitation energies of the 3^- state in Ni and Zn isotopes have the similar trends of smoothly decreasing energy with increasing neutron number and have the minimum energies at $N = 40$ and 38, respectively. This picture suggests that the strong octupole effects occurring around 38, 40 likely give rise to the enhanced $E3$ transitions in the neighboring odd-Z isotones. The experimental $B(E3)/B(E1)$ branching ratio in ^{67}Ga is extracted. The deduced value of $4.58(22) \times 10^7$ fm^4 in ^{67}Ga is close to the $7.60(89) \times 10^7$ fm^4 in ^{69}Cu and smaller than the $2.62(4) \times 10^9$ fm^4 in ^{67}Cu. According to the available experimental half-lives of 1.04–6.9 ps for the $9/2^+$ states in ^{67}Ga [21,22], the $B(E3)$ values are deduced to be between 9.2–61.1 W.u., which is also on the same level as the $B(E3)$ value of >11.2 W.u. in ^{67}Cu.

To further investigate the octupole properties in ^{67}Ga, the RAT-PRM [8,9] and RMF+BCS [10–12] calculations have been performed. The RAT-PRM has been successfully applied to investigate the parity doublet bands [25–28], multiple chiral doublets with octupole correlations [8,9,29,30], and the predicted chirality-parity quartet bands [31], while the RMF+BCS has been successfully applied to study the octupole deformation or correlations in nuclei [10,32–34].

The quadrupole deformation parameters in the present RAT-PRM calculations are taken from Ref. [35], i.e., $\beta_2 = 0.185$ and $\gamma = 32.5^\circ$ for ^{67}Ga. As no static octupole deformation is found in the microscopic PES shown in Fig. 8, the octupole deformation parameter $\beta_3 = 0$ is adopted. To further probe the effect of octupole deformation, the RAT-PRM calculations with $\beta_3 = 0.02$, 0.04, 0.06, and 0.08 are also performed for comparison. With these deformation parameters, the reflection-asymmetric Nilsson Hamiltonian with the parameters κ, μ in Ref. [36] is solved in the harmonic-oscillator basis [37]. The proton Fermi energy $\lambda_p = 47.69$ MeV is

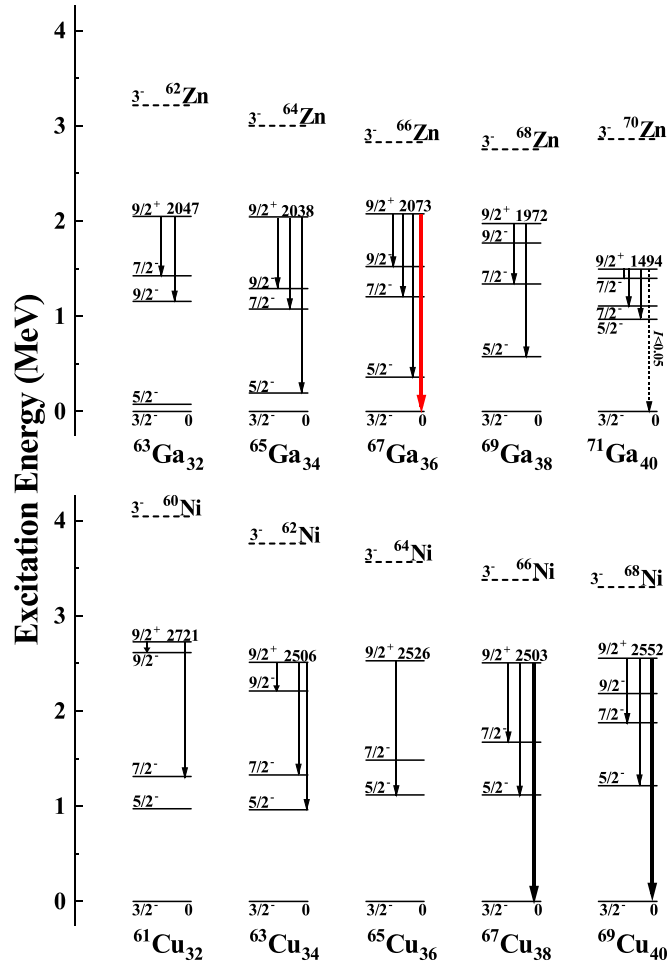

FIG. 6. Low-lying states and the transitions populated by the $9/2^+$ states in odd-Z $^{63-71}$Ga and $^{61-69}$Cu isotopes. The 3^- octupole states in the even-Z Zn and Ni isotopes are indicated by dashed lines. The newly observed $E3$ transition in ^{67}Ga is marked as red.

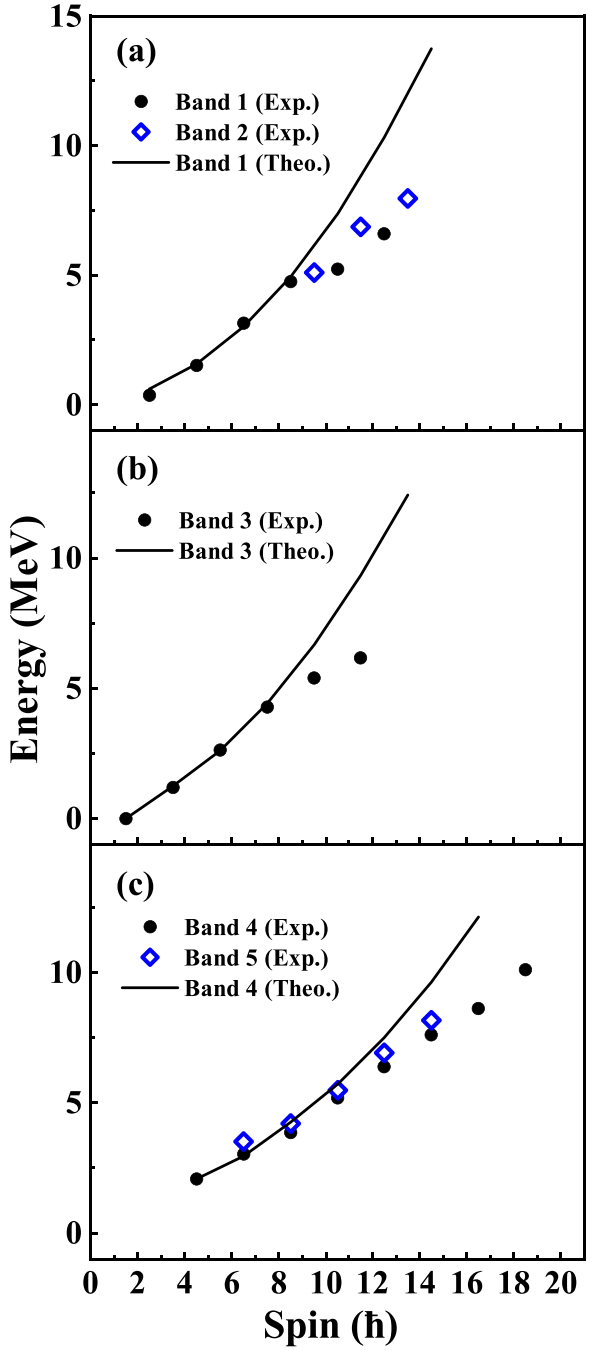

FIG. 7. The calculated energy spectra of the negative-parity bands 1 and 3, and the positive-parity band 4 by the RAT-PRM (labeled as "Theo."), in comparison with the available data. The experimental energy spectra of the negative-parity band 2 and positive-parity band 5 are also shown.

chosen to correspond to the orbital $\pi p_{3/2}[\Omega = 3/2]$, and the pairing gap follows the empirical formula $\Delta = 12/\sqrt{A}$ MeV. The single-particle space available to the odd proton is truncated to 13 levels with six above and six below the Fermi level. For the core part, the configuration-dependent moments of inertia [30] with $\mathcal{J}_0 = 11\hbar^2/\text{MeV}$ for positive parity band and $8\hbar^2/\text{MeV}$ for negative parity band are adopted. The

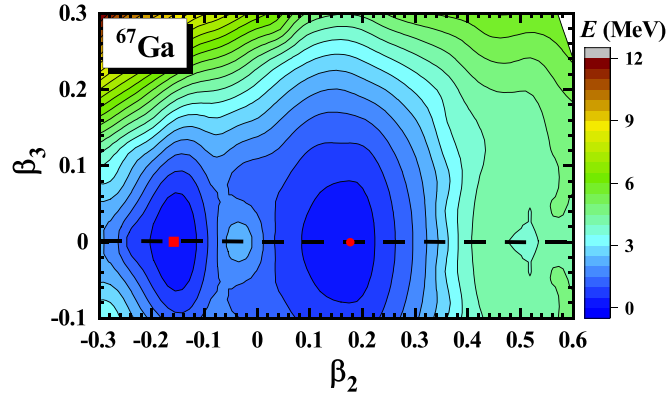

FIG. 8. The potential-energy surfaces for ^{67}Ga calculated by the RMF+BCS model. The filled circle and square correspond to the positions of the ground state and second minimum, respectively. The contour separation is 0.5 MeV.

core parity splitting parameter $E(0^-) = 3.0$ MeV is used. For the calculations of the electric transition probabilities, the empirical intrinsic dipole moment $Q_{10} = \frac{3}{4\pi}R_0 Z\beta_{10}$ and quadrupole moment $Q_0 = \frac{3}{\sqrt{5\pi}}R_0^2 Z\beta_2$ are used with $R_0 = 1.2A^{1/3}$ fm [8].

Figure 7 shows the energy spectra of the negative-parity bands 1 and 3 as well as the positive-parity band 4 calculated by the RAT-PRM, in comparison with the available data. As shown in Fig. 7, the experimental spectra of these bands are well reproduced by the RAT-PRM in the low spin region. The deviations in the high spin region result from the three-quasiparticle alignment which has not been considered in the present RAT-PRM calculations. The main components of the intrinsic wave functions in the RAT-PRM are found to be $\pi f_{5/2}$ for band 1, $\pi p_{3/2}$ for band 3, and $\pi g_{9/2}$ for band 4, which are consistent with the experimental systematics in this region [16–19]. The energy spectra as functions of spin for bands 2 and 5 are also plotted in Figs. 7(a) and 7(c), respectively. Their features are similar to those of bands 1 and 4, respectively, which suggest bands 2 and 5 may also have similar proton configurations to bands 1 and 4, respectively.

The potential energy surface (PES) on the (β_2, β_3) plane for ^{67}Ga calculated by the RMF+BCS is shown in Fig. 8. It can be seen that the ground state of ^{67}Ga corresponds to the reflection symmetric shape, but the PES around the ground state is soft along the direction of β_3.

It is known that in this region rotation tends to drive octupole-soft nuclei to static octupole deformation at high angular momenta [38]. Therefore, investigation on the effect of rotation on the octupole correlations in ^{67}Ga is interesting. In Table II, the calculated $B(E1)/B(E2)$ ratios between the interband $E1$ transitions (band $3 \rightarrow 4$) and the intraband $E2$ transitions (band 3) at spin $19/2^-\hbar$ by RAT-PRM are shown in comparison with the experimental data measured in this work. It can be seen that the RAT-PRM calculation with $\beta_3 = 0.0$ results in an underestimation of the $B(E1)/B(E2)$ ratio at $19/2^-\hbar$. By increasing β_3 from 0.0 to 0.08, we find that the octupole deformation sensitively affects the calculated

TABLE II. The calculated $B(E1)/B(E2)$ ratios between the interband $E1$ transitions (band $3 \rightarrow 4$) and the intraband $E2$ transitions (band 3) at spin $19/2^-\hbar$ by RAT-PRM in comparison with the experimental data measured in this work.

		$B(E1)/B(E2)$ (10^{-6} fm^{-2})	
I_i^π	β_3	Theo.	Expt.
$19/2^-$	0.00	0.527	1.055(70)
	0.02	0.321	
	0.04	0.003	
	0.06	0.843	
	0.08	1.278	

$B(E1)$ values, while it has no significant influence on the energy spectra and the $B(E2)$ values. As seen in Table II, with β_3 from 0.0 to 0.08, the calculated $B(E1)/B(E2)$ ratio at $19/2^-\hbar$ first decreases and then increases, and can achieve a good agreement with the experimental data when $\beta_3 = 0.06$ or $\beta_3 = 0.08$. The nonmonotonic change of the calculated $B(E1)$ value with the increase of β_3 is owing to the interplay between contributions from the collective core and the valence particles to the transitional probabilities [39]. The $E1$ transition operator contains two terms from the collective core and the valence particles, respectively. When $\beta_3 = 0.0$, the $B(E1)$ value is totally determined from the valence particle part. When β_3 increases, the collective core part starts to contribute and interacts with the valence particle part, which will finally dominate the $B(E1)$ value with very large β_3. Nevertheless, the agreement achieved here at a large β_3 indicates that the static octupole deformation might appear at high spins for the negative parity band 3. Presently the experimental information on the octupole correlation at high spin in ^{67}Ga is limited. More experimental studies are anticipated.

IV. SUMMARY

High-spin states of ^{67}Ga have been studied via the ^{58}Ni(^{12}C, $3p$)^{67}Ga fusion-evaporation reaction at a beam energy of 50.4 MeV. Three negative-parity bands and three positive-parity bands in ^{67}Ga are established. The observation of one new $E3$ transition and several $E1$ transitions linking the positive-parity $\pi 1g_{9/2}$ band and negative-parity $\pi 2p_{3/2}$ band provides evidence of octupole correlations in ^{67}Ga. Systematic of the excitation energies of the 3^- state in Ni and Zn isotopes and observation of the enhanced $E3$ transitions in ^{67}Ga and ^{67,69}Cu indicate that the strong octupole effects in the $Z = 28$–30 region may occur around neutron number 38 and 40.

The characteristics of octupole correlations in the ^{67}Ga are discussed in terms of the RAT-PRM and RMF+BCS. At low angular momenta, the ^{67}Ga is found to be soft with respect to the reflection-asymmetric shape. With the increase in angular momentum, its reflection-asymmetry shape might be developed. To have a complete picture in octupole correlations in this mass region, more experimental studies, like searching the $E3$ transitions in ^{69,71}Ga, identifying the 3^- states in ^{70}Ni and ^{72}Zn, investigating the evolution of octupole correlation with spin, are highly desired.

ACKNOWLEDGMENTS

This work was supported by the National Key R&D Program of China under Grants No. 2022YFA1602302 and No. 2018YFA0404403, the National Natural Science Foundation of China under Grants No. 12035001, No. 12075006, No. U2167201, No. 12205097, No. 12070131001, and No. 11935003, the Fundamental Research Funds for the Central Universities (Grant No. 2022MS051), and the State Key Laboratory of Nuclear Physics and Technology, Peking University (Grant No. NPT2023ZX01).

[1] I. Ahmad and P. A. Butler, Octupole shapes in nuclei, Annu. Rev. Nucl. Part. Sci. **43**, 71 (1993).

[2] P. A. Butler and W. Nazarewicz, Intrinsic reflection asymmetry in atomic nuclei, Rev. Mod. Phys. **68**, 349 (1996).

[3] L. P. Gaffney, P. A. Butler, M. Scheck, A. B. Hayes, F. Wenander, M. Albers, B. Bastin, C. Bauer, A. Blazhev, S. Bönig, N. Bree, J. Cederkäll, T. Chupp, D. Cline, T. E. Cocolios, T. Davinson, H. De Witte, J. Diriken, T. Grahn, A. Herzan *et al.*, Studies of pear-shaped nuclei using accelerated radioactive beams, Nature (London) **497**, 199 (2013).

[4] B. Bucher, S. Zhu, C. Y. Wu, R. V. F. Janssens, D. Cline, A. B. Hayes, M. Albers, A. D. Ayangeakaa, P. A. Butler, C. M. Campbell, M. P. Carpenter, C. J. Chiara, J. A. Clark, H. L. Crawford, M. Cromaz, H. M. David, C. Dickerson, E. T. Gregor, J. Harker, C. R. Hoffman *et al.*, Direct evidence of octupole deformation in neutron-rich ^{144}Ba, Phys. Rev. Lett. **116**, 112503 (2016).

[5] B. Bucher, S. Zhu, C. Y. Wu, R. V. F. Janssens, R. N. Bernard, L. M. Robledo, T. R. Rodríguez, D. Cline, A. B. Hayes, A. D. Ayangeakaa, M. Q. Buckner, C. M. Campbell, M. P. Carpenter, J. A. Clark, H. L. Crawford, H. M. David, C. Dickerson, J. Harker, C. R. Hoffman, B. P. Kay *et al.*, Direct evidence for octupole deformation in ^{146}Ba and the origin of large $E1$ moment variations in reflection-asymmetric nuclei, Phys. Rev. Lett. **118**, 152504 (2017).

[6] C. Liu, S. Y. Wang, R. A. Bark, S. Q. Zhang, J. Meng, B. Qi, P. Jones, S. M. Wyngaardt, J. Zhao, C. Xu, S.-G. Zhou, S. Wang, D. P. Sun, L. Liu, Z. Q. Li, N. B. Zhang, H. Jia, X. Q. Li, H. Hua, Q. B. Chen *et al.*, Evidence for octupole correlations in multiple chiral doublet bands, Phys. Rev. Lett. **116**, 112501 (2016).

[7] C. G. Wang, R. Han, C. Xu, H. Hua, R. A. Bark, S. Q. Zhang, S. Y. Wang, T. M. Shneidman, S. G. Zhou, J. Meng, S. M. Wyngaardt, A. C. Dai, F. R. Xu, X. Q. Li, Z. H. Li, Y. L. Ye, D. X. Jiang, C. G. Li, C. Y. Niu, Z. Q. Chen *et al.*, First evidence of an octupole rotational band in Ge isotopes, Phys. Rev. C **106**, L011303 (2022).

[8] Y. Y. Wang, S. Q. Zhang, P. W. Zhao, and J. Meng, Multiple chiral doublet bands with octupole correlations in reflection-asymmetric triaxial particle rotor model, Phys. Lett. B **792**, 454 (2019).

[9] Y. P. Wang, Y. Y. Wang, and J. Meng, Pseudospin symmetry and octupole correlations for multiple chiral doublets in ^{131}Ba, Phys. Rev. C **102**, 024313 (2020).

[10] W. Zhang, Z. P. Li, S. Q. Zhang, and J. Meng, Octupole degree of freedom for the critical-point candidate nucleus ^{152}Sm in a reflection-asymmetric relativistic mean-field approach, Phys. Rev. C **81**, 034302 (2010).

[11] S. Y. Xia, H. Tao, Y. Lu, Z. P. Li, T. Nikšić, and D. Vretenar, Spectroscopy of reflection-asymmetric nuclei with relativistic energy density functionals, Phys. Rev. C **96**, 054303 (2017).

[12] B. Wei, Q. Zhao, Z. H. Wang, J. Geng, B. Y. Sun, Y. F. Niu, and W. H. Long, Novel relativistic mean field Lagrangian guided by pseudo-spin symmetry restoration, Chin. Phys. C **44**, 074107 (2020).

[13] D. Radford, ESCL8R and LEVIT8R: Software for interactive graphical analysis of HPGe coincidence data sets, Nucl. Instrum. Methods Phys. Res. A **361**, 297 (1995).

[14] J. Dudouet, Cubix (1.0), Zenodo (2024), https://doi.org/10.5281/zenodo.10683242.

[15] M. Piiparinen, A. Ataç, J. Blomqvist, G. Hagemann, B. Herskind, R. Julin, S. Juutinen, A. Lampinen, J. Nyberg, G. Sletten, P. Tikkanen, S. Törmänen, A. Virtanen, and R. Wyss, High-spin spectroscopy of the ^{142}Eu, ^{143}Eu and ^{144}Eu nuclei, Nucl. Phys. A **605**, 191 (1996).

[16] S. Zhu, L. Chaturvedi, J. H. Hamilton, A. V. Ramayya, C. Girit, J. Kormicki, X. W. Zhao, W. B. Gao, N. R. Johnson, I. Y. Lee, C. Baktash, F. K. McGowan, M. L. Halbert, M. Riley, M. O. Kortelahti, and J. D. Cole, High spin states in ^{65}Ga, ^{67}Ga and their collective behavior at high angular momenta, Chin. J. Nucl. Phys. **13**, 331 (1991).

[17] I. Dankó, D. Sohler, Z. Dombrádi, S. Brant, V. Krstić, J. Cederkäll, M. Lipoglavšek, M. Palacz, J. Persson, A. Atac, C. Fahlander, H. Grawe, A. Johnson, A. Kerek, W. Klamra, J. Kownacki, A. Likar, L.-O. Norlin, J. Nyberg, V. Paar *et al.*, Collective and broken pair states of ^{65,67}Ga, Phys. Rev. C **59**, 1956 (1999).

[18] I. Stefanescu, W. B. Walters, R. V. F. Janssens, S. Zhu, R. Broda, M. P. Carpenter, C. J. Chiara, B. Fornal, B. P. Kay, F. G. Kondev, W. Krolas, T. Lauritsen, C. J. Lister, E. A. McCutchan, T. Pawlat, D. Seweryniak, J. R. Stone, N. J. Stone, and J. Wrzesinski, Identification of the $g_{9/2}$-proton bands in the neutron-rich ^{71,73,75,77}Ga nuclei, Phys. Rev. C **79**, 064302 (2009).

[19] U. S. Ghosh, B. Mukherjee, and S. Rai, Shell model study of nuclear structure in ^{63,65,67}Ga, Int. J. Mod. Phys. E **29**, 2050045 (2020).

[20] L. Harms-Ringdahl, J. Sztarkier, and Z. P. Sawa, On $1f2p$ nuclei. search for the particle-plus-core excitation mode in ^{65}Ga, ^{67}Ga and ^{69}Ga, Phys. Scr. **9**, 15 (1974).

[21] A. M. Al-Naser, A. H. Behbehani, L. L. Green, C. J. Lister, P. J. Nolan, and J. F. Sharpey-Schafer, The structure of levels in ^{67}Ga below 2.5 MeV excitation, J. Phys. G **3**, 1383 (1977).

[22] A. M. Al-Naser, A. H. Behbehani, L. L. Green, A. N. James, C. J. Lister, P. J. Nolan, N. Rammo, J. F. Sharpey-Schafer, L. Zybert, and R. Zybert, Gamma-ray spectroscopy of high-spin levels in ^{67}Ga, J. Phys. G **4**, 1611 (1978).

[23] V. Zobel, L. Cleemann, J. Eberth, W. Neumann, and N. Weihl, High spin states in ^{67}Ga, Nucl. Phys. A **316**, 165 (1979).

[24] H. Junde, X. L. Huang, and J. Tuli, Nuclear data sheets for A = 67, Nucl. Data Sheets **106**, 159 (2005).

[25] C. Morse, A. O. Macchiavelli, H. L. Crawford, S. Zhu, C. Y. Wu, Y. Y. Wang, J. Meng, B. B. Back, B. Bucher, C. M. Campbell, M. P. Carpenter, J. Chen, R. M. Clark, M. Cromaz, P. Fallon, J. Henderson, R. V. F. Janssens, M. D. Jones, T. L. Khoo, F. G. Kondev *et al.*, Quadrupole and octupole collectivity in ^{143}Ba, Phys. Rev. C **102**, 054328 (2020).

[26] S. Rajbanshi, R. Palit, R. Raut, Y. Y. Wang, Z. X. Ren, J. Meng, Q. B. Chen, S. Ali, H. Pai, F. S. Babra, R. Banik, S. Bhattacharya, S. Bhattacharyya, P. Dey, S. Malik, G. Mukherjee, M. S. R. Laskar, S. Nandi, R. Santra, T. Trivedi *et al.*, Evidence of octupole correlation in ^{79}Se, Phys. Rev. C **104**, 064316 (2021).

[27] Y. Y. Wang, Parity doublet bands in ^{223}Th within reflection-asymmetric triaxial particle rotor model, Phys. Rev. C **104**, 014318 (2021).

[28] Y. Y. Wang, Q. B. Chen, and S. Q. Zhang, Interpretation of enhanced electric dipole transitions in ^{73}Br by the reflection-asymmetric triaxial particle rotor model, Phys. Rev. C **105**, 044316 (2022).

[29] S. Guo, C. M. Petrache, D. Mengoni, Y. H. Qiang, Y. P. Wang, Y. Y. Wang, J. Meng, Y. K. Wang, S. Q. Zhang, P. W. Zhao, A. Astier, J. G. Wang, H. L. Fan, E. Dupont, B. F. Lv, D. Bazzacco, A. Boso, A. Goasduff, F. Recchia, D. Testov *et al.*, Evidence for pseudospin-chiral quartet bands in the presence of octupole correlations, Phys. Lett. B **807**, 135572 (2020).

[30] Y. Y. Wang and S. Q. Zhang, Interpretation of chiral symmetry breaking and octupole correlations in ^{124}Cs by the reflection-asymmetric triaxial particle rotor model, Phys. Rev. C **102**, 034303 (2020).

[31] Y. Y. Wang, X. H. Wu, S. Q. Zhang, P. W. Zhao, and J. Meng, Selection rules of electromagnetic transitions for chirality-parity violation in atomic nuclei, Sci. Bull. **65**, 2001 (2020).

[32] Z. Xu and Z. P. Li, Microscopic analysis of octupole shape transitions in neutron-rich actinides with relativistic energy density functional, Chin. Phys. C **41**, 124107 (2017).

[33] W. Zhang and Y. F. Niu, Shape transition with temperature of the pear-shaped nuclei in covariant density functional theory, Phys. Rev. C **96**, 054308 (2017).

[34] W. Zhang, Z. P. Li, and S. Q. Zhang, Octupole deformation for Ba isotopes in a reflection-asymmetric relativistic mean-field approach, Chin. Phys. C **34**, 1094 (2010).

[35] P. Möller, R. Bengtsson, B. Carlsson, P. Olivius, T. Ichikawa, H. Sagawa, and A. Iwamoto, Axial and reflection asymmetry of the nuclear ground state, At. Data Nucl. Data Tables **94**, 758 (2008).

[36] S. G. Nilsson, C. F. Tsang, A. Sobiczewski, Z. Szymański, S. Wycech, C. Gustafson, I.-L. Lamm, P. Möller, and B. Nilsson, On the nuclear structure and stability of heavy and superheavy elements, Nucl. Phys. A **131**, 1 (1969).

[37] Y. Y. Wang and Z. X. Ren, Single particles in a reflection-asymmetric potential, Sci. China Phys. Mech. Astron. **61**, 082012 (2018).

[38] P. D. Cottle, Possible static octupole deformation at high angular momentum in ^{78}Kr and ^{126,128}Ba, Phys. Rev. C **41**, 517 (1990).

[39] G. Leander, W. Nazarewicz, G. Bertsch, and J. Dudek, Low-energy collective E1 mode in nuclei, Nucl. Phys. A **453**, 58 (1986).